

Mid-infrared dual-comb polarimetry of anisotropic samples

Karsten Hinrichs¹  | Brianna Blevins^{2,3} | Andreas Furchner⁴ |
Nataraja Sekhar Yadavalli^{2,3} | Sergiy Minko^{2,3,5} | Raphael Horvath⁶ |
Markus Mangold⁶

¹Leibniz-Institut für Analytische Wissenschaften – ISAS – e.V., Berlin, Germany

²Nanostructured Materials Laboratory, The University of Georgia, Athens, Georgia, USA

³Department of Chemistry, The University of Georgia, Athens, Georgia, USA

⁴Helmholtz-Zentrum Berlin für Materialien und Energie, Division Energy and Information, Berlin, Germany

⁵Department of Textile, Merchandising and Interiors, The University of Georgia, Athens, Georgia, USA

⁶IRsweep AG, Staefa, Switzerland

Correspondence

Karsten Hinrichs, Leibniz-Institut für Analytische Wissenschaften – ISAS – e.V., Schwarzschildstraße 8, 12489 Berlin, Germany.
Email: karsten.hinrichs@isas.de

Funding information

Die Regierende Bürgermeisterin von Berlin – Senatsverwaltung Wissenschaft; Gesundheit, Pflege und Gleichstellung; Ministerium für Innovation, Wissenschaft und Forschung des Landes Nordrhein-Westfalen; Federal Ministry of Education and Research, Grant/Award Number: 03EW0015A/B; European Union, Grant/Award Numbers: EFRE 1.8/13, Horizon 2020 grant 820419

Abstract

The mid-infrared (mid-IR) anisotropic optical response of a material probes vibrational fingerprints and absorption bands sensitive to order, structure, and direction-dependent stimuli. Such anisotropic properties play a fundamental role in catalysis, optoelectronic, photonic, polymer and biomedical research and applications. Infrared dual-comb polarimetry (IR-DCP) is introduced as a powerful new spectroscopic method for the analysis of complex dielectric functions and anisotropic samples in the mid-IR range. IR-DCP enables novel hyperspectral and time-resolved applications far beyond the technical possibilities of classical Fourier-transform IR approaches. The method unravels structure–spectra relations at high spectral bandwidth up to 90 cm^{-1} and short integration times of $65\ \mu\text{s}$, with previously unattainable time resolutions for spectral IR polarimetric measurements for potential studies of noncyclic and irreversible processes. The polarimetric capabilities of IR-DCP are demonstrated by investigating an anisotropic inhomogeneous freestanding nanofiber scaffold for neural tissue applications. Polarization sensitive multi-angle dual-comb transmission amplitude and absolute phase measurements (separately for ss-, pp-, ps-, and sp-polarized light) allow the in-depth probing of the samples' orientation-dependent vibrational absorption properties. Mid-IR anisotropies can quickly be identified by cross-polarized IR-DCP polarimetry.

Key points

- A novel dual-comb laser-based technique is established for polarization-dependent mid-infrared spectroscopy.
- Independent measurements of spectral s- and p-polarized transmission amplitudes and phases in the μs range.
- Visualization of the anisotropy of nanofiber scaffolds as used for neural tissue applications.

This is an open access article under the terms of the [Creative Commons Attribution](https://creativecommons.org/licenses/by/4.0/) License, which permits use, distribution and reproduction in any medium, provided the original work is properly cited.

© 2023 The Authors. *Natural Sciences* published by Wiley-VCH GmbH.

KEYWORDS

anisotropy, dual-comb spectroscopy, infrared laser, mid-infrared spectroscopy, nanofiber, polarimetry, sensing

INTRODUCTION

The anisotropy of materials is associated, for example, with direction-dependent optical, mechanical, physical, and chemical properties.^{1–7} Anisotropy plays a key role in optoelectronic, photonic, polymer, catalytic and bio-related research, and applications. Specific examples are the design and engineering of optical devices,^{1–4} two-dimensional (2D) materials,³ and touch-spun nanofibers for nerve regeneration,⁷ the latter of which are studied in this work. For the analysis of anisotropic material properties, infrared (IR) methods are prominently used, as these probe material and structural properties in a contactless manner in various environments with high sensitivity.

Driven by the tremendous application potential in scientific and industrial applications, numerous IR spectroscopies were developed in recent years. Classical IR spectroscopies are workhorses in many labs. However, it is not possible to simultaneously measure the real and imaginary part of complex transmissions or reflections. To satisfy this demand, polarimetric or ellipsometric IR spectroscopic methods have to be developed for the respective application fields. This challenge can be solved by introducing innovative measurement concepts, implementing new radiation sources, and realizing novel hyperspectral or imaging measurement schemes.

Recent rapidly developing IR spectroscopic methods based on quantum cascade lasers (QCLs) are heralding a new era in IR spectroscopic analytics with a plethora of new applications far beyond the possibilities of Fourier-transform IR (FTIR) spectroscopy.^{8–17} These methods nowadays offer high spectral resolutions in laboratory and field applications while providing high optical throughput, sub-millimeter spot sizes, and sub-second temporal resolution for sensing applications, time-resolved studies, as well as hyperspectral imaging. Of particular interest for structural and chemical analyses of interfaces, aggregates, thin films, and structured materials are polarization-dependent QCL-based methods, such as AFM-IR,^{18,19} IR nanoscopy,²⁰ antenna-assisted IR nano-spectroscopy,²¹ IR microscopy,^{22,23} polarimetric IR-ATR,²⁴ vibrational circular dichroism,²⁵ far-field optical photothermal IR,²⁶ and IR spectroscopic ellipsometry/polarimetry.^{10,11,27–29}

In 2016/2017, the dual-comb spectroscopic technique³⁰ was combined with polarization-dependent measurements.^{31,32} So-called spectroscopic dual-comb ellipsometry³² in the near-IR spectral range of 1514–1595 nm became available. The authors³² already anticipated a transfer of the method to the mid-IR and far-IR region, which would enable future applications for studies of materials with IR active transitions. In this work, we fulfill these expectations and introduce QCL-based IR dual-comb polarimetry (IR-DCP) as a novel technique for temporally (sub-millisecond) and spectrally (1.4 cm^{-1}) highly resolved

investigations of anisotropic sample properties in the mid-IR spectral range.

Polarimetric methods

Figure 1 shows schematic designs of IR-DCP (a) and classical FTIR polarimetry (b). Both methods aim to probe the spectral function of the polarization-dependent complex transmission (reflection) coefficients, in general defined as $t_{xy} = |t_{xy}| \cdot \exp(i\Delta_{xy})$ [y-polarized light in, x-polarized light out, Δ is the phase], are sensitive to the transmission $T_{xy} = |t_{xy}|^2$. Classical FTIR polarimetry can acquire relative phases for two sets of polarization configurations, such as $\Delta_{xx} - \Delta_{yy}$. For the presented experiments, light polarized at 0° and 90° is considered for the beam before and after the sample. To avoid confusion with the sample azimuthal settings in degrees ($0^\circ =$ horizontal orientation; $90^\circ =$ vertical orientation), we use the following notation for polarizer/analyzer settings: (i) ss for parallel polarizers in horizontal direction, (ii) pp for parallel polarizers in vertical direction, (iii) sp and ps for crossed polarizers. For FTIR polarimetric studies of materials with $\cos \Delta \approx 1$ (Δ close to 0 or π), a retarder is required as an additional optical element to achieve sufficiently high accuracy. In contrast, IR-DCP can directly measure absolute phases Δ_{xy} .

The dual-comb system (IRis-F1, IRsweep AG, Switzerland, schematic in Figure 1a) comprises two QCL frequency combs (FC 1 and FC 2). FC 1 probes the sample, whereas FC 2 works as the local oscillator. For this experiment, polarizers (P1, P2, P3, BaF₂, part number GS57502, Specac, England, extinction ratio of 400:1 @ 1000 cm^{-1}) and beamsplitters (ZnSe, part number BSW710, Thorlabs) are used for controlling incident and output power and polarization states, as well as beam propagation and recombination. P1 regulates the incident power (typically about 0.75 mW at the sample), P2 sets the incident polarization, and P3 acts as an analyzer. Further polarizers (not shown) control the power incident on the reference detector and ensure polarization matching of local oscillator beam and sample beam. The sample was placed between P2 and P3 on a rotational mount. The beam diameter at the sample position was about 3 mm (FWHM, Gauss).

The operating principles of dual-comb spectroscopy have been described previously.^{35–37} Briefly, FC 1 and FC 2 deliver frequency combs with interline spacings ($f_{\text{rep},1}$ and $f_{\text{rep},2}$) of about 10 GHz and optical coverage of up to 90 cm^{-1} (typically $60\text{--}80\text{ cm}^{-1}$).³⁸ When FC 1 and FC 2 are overlaid on a high-bandwidth mercury-cadmium-telluride (MCT) detector, a heterodyne beating corresponding to $\Delta f_{\text{rep}} = f_{\text{rep},1} - f_{\text{rep},2} \approx 2\text{ MHz}$ can be recorded in the time-domain. Conducting a Fourier transform on this signal allows for the individual

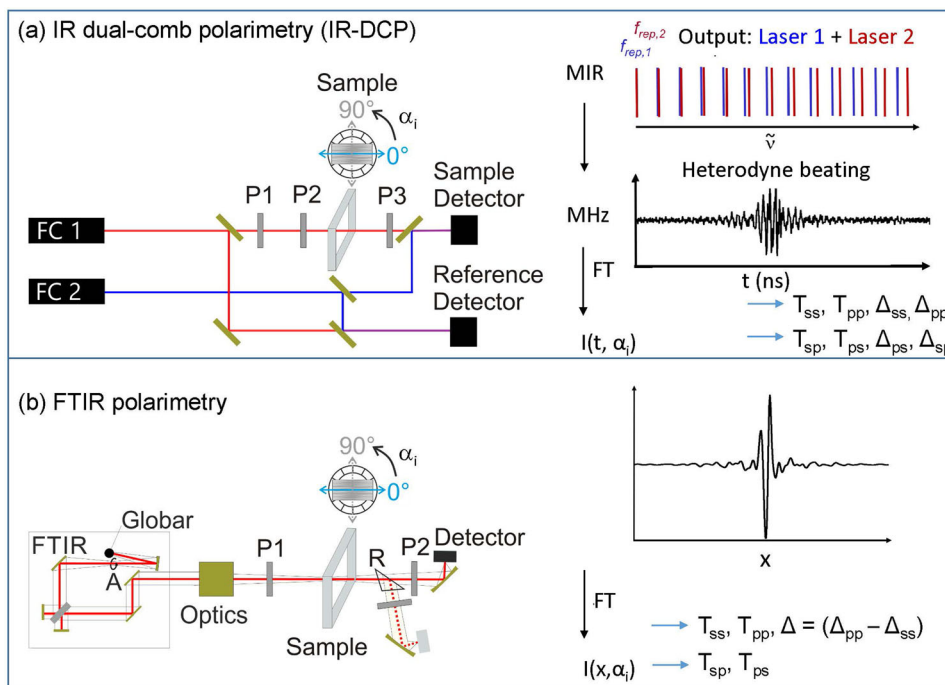


FIGURE 1 Schematic setups of (a) IR dual-comb polarimetry (IR-DCP) and (b) Fourier-transform IR (FTIR) polarimetry. The measurement principle is outlined on the right side. Typical measurement parameters are parallel-polarized (ss, pp) and cross-polarized (sp, ps) transmissions T_{xy} (reflections R_{xy}) and absolute phases Δ_{xy} or relative phases Δ in dependence of the azimuthal angle (α_i). See text for further methodical details.

frequency contributions to be resolved. The reference detector is used to correct for amplitude and frequency noise of the free-running QCLs. For a given polarizer configuration, measuring the difference between a setup without (background measurement) and one with a sample (sample measurement) gives the complex transmission t_{xy} , the angle of which yields the absolute phase. The theoretical time resolution is $1/\Delta f_{\text{rep}}$ ^{37,39}; however, for data-handling and signal-to-noise reasons, the spectrometer is typically operated at a time resolution of 4 μs .^{37,39} In the present study, the integration time was 65 μs . A transmission geometry at 0° incidence angle was used. Note that, for non-depolarizing samples, the ss-, pp-, sp-, and ps-polarized measurements are directly related to the Jones matrix and specific combinations of the respective Mueller-matrix elements,⁴⁰ which enables the analysis of complex dielectric functions (real and imaginary part).⁴¹

The FTIR polarimeter (Figure 1b) is coupled to an FTIR IFS 55 spectrometer (BRUKER, Germany) serving as a radiation source. A Jacquinot aperture (A) of 1.85 mm results in a spot size on the sample of about 4.5 mm (FWHM). The sample was placed on a rotational mount. Polarizers (KRS5, Specac, England; extinction ratio of 148:1 @ 1000 cm^{-1}) P1 and P2 act as polarizer and analyzer, respectively. A liquid-nitrogen-cooled photovoltaic MCT detector (Kolmar Technologies, Newburyport, MA, USA) was used. A retarding element (R) was additionally inserted for sensitive phase measurements. The opening angle was about $\pm 3.5^\circ$. Measured experimental quantities are the relative phase $\Delta = \Delta_{\text{pp}} - \Delta_{\text{ss}}$ and the polarization-dependent transmission $T_{\text{pp}} = |t_{\text{pp}}|^2$ and $T_{\text{ss}} = |t_{\text{ss}}|^2$ at 0° incidence angle. $|t_{\text{pp}}|$ and $|t_{\text{ss}}|$ represent the amplitudes of the respective pp- and ss-polarized complex trans-

mission coefficients (for incidence angles larger than 0° , p is parallel, and s is perpendicular to the optical incidence plane), and Δ is the phase shift between them. Further details are found in Refs. [33, 41] for the ellipsometric method and in Ref. [33] for the employed setup.

MATERIALS

A nanofiber scaffold was prepared via the touch-spinning method in a freestanding manner on a wire collector from 8% polycaprolactone (PCL, $M_n = 80,000\text{ g/mol}$, Sigma-Aldrich) in chloroform (ACS grade, VWR Chemicals BDH). Details on touch-spinning can be found in Ref. [7]. The fibers were exposed to a 0.1% bovine serum albumin solution.

Anisotropic nanofiber scaffold

Figure 2 shows polarization-dependent transmission and phase spectra of the nanofiber sample for 0° and 90° azimuthal rotation. The observed band at about 1240 cm^{-1} is assigned to the asymmetric C–O–C stretching vibration (according to Ref. [42]) of the PCL chain. The onset of a second vibrational band at about 1293 cm^{-1} is observed at the edge of the investigated spectral range. Qualitative agreement in band position, amplitude, and shape is found for the band at 1240 cm^{-1} between the corresponding sets of polarized transmission IR-DCP and FTIR polarimetric spectra. For the onset of a band around 1293 cm^{-1} , good qualitative agreement is found for most of the polarized

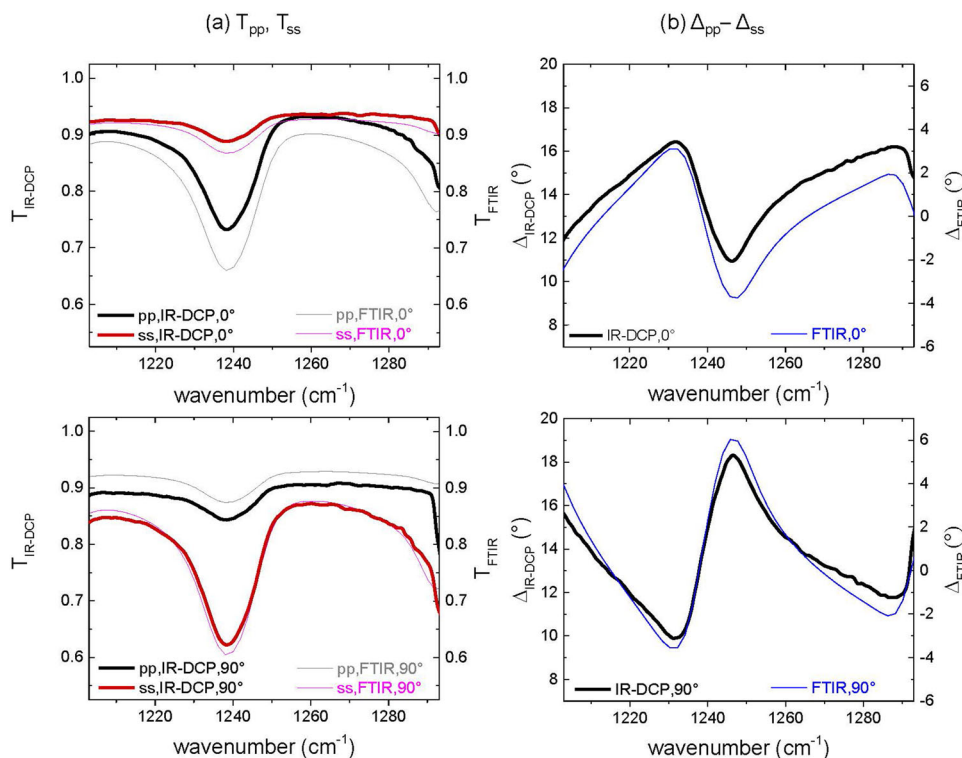


FIGURE 2 (a) T_{pp} and T_{ss} from infrared dual-comb polarimetry (IR-DCP) and Fourier-transform IR (FTIR) polarimetry at 0° (top) and 90° (bottom) azimuthal sample rotation. (b) Corresponding polarized relative phase spectra from IR-DCP and FTIR polarimetry

transmission spectra and both types of phase spectra. Somewhat stronger differences are observed around 1293 cm⁻¹ for the pp-polarized spectra at 90° azimuth because of a higher noise level toward the edge of the measurement window.

A strong anisotropy is identified in the range of the C–O–C vibrational band. This anisotropy originates from the direction-dependent vibrational absorption due to the predominant alignment of polymer chains within single fibers, but also due to the overall close-to-parallel orientation of the individual fibers.^{43,44} Qualitative agreement is observed between the relative phase spectra obtained from IR-DCP and FTIR polarimetry (Figure 2b).

Differences in the band amplitudes in the transmission and phase spectra of IR-DCP and FTIR are larger at 0° compared to 90° azimuthal angle. Such differences could be related to the inhomogeneity of the fiber scaffold and the different sizes and opening angles of the probe beam in IR-DCP and FTIR. However, band positions and shapes agree well for both methods. Indeed, the relative phase spectra exhibit the expected Kramers–Kronig consistent line shape, thus demonstrating the validity of the method.

The recorded IR-DCP and FTIR polarimetric relative phases show a constant offset of approximately 13°. Its likely origin is the adjustment of incident power via P1 between the Δ_{pp} and Δ_{ss} measurements necessitated by a change in the input polarization. For future measurements, an invariant P1 is recommended, for example, by setting P1 to 45° and controlling the power through neutral density filters.

Figure 3a shows images of ss- and sp-polarized transmission and absolute phase spectra versus sample azimuth in 10° steps. Maximum

band intensities in the T_{ss} images (corresponding to a minimum in T_{ss}) are observed around 90° azimuth, whereas maximum band intensities in T_{sp} (corresponding to a maximum of T_{sp}) are seen at 45° azimuth. The average orientation of transition dipole moments of the related C–O–C vibrational band is therefore aligned predominantly in the direction of the fibers, in agreement with the overall predominant alignment of the fibers in the scaffold. Note that the baseline in regions of weak anisotropy beside the bands can be significantly modified by polarizer leakage in cross-polarized spectra.⁴⁵

The parallel-polarized T_{ss} and Δ_{ss} images capture all vibrational contributions along the ss polarization axis and therefore also include isotropic contributions. In contrast, the cross-polarized T_{sp} and Δ_{sp} images are only sensitive to signals from anisotropic contributions, qualifying them for the direct inspection of anisotropies. The anisotropic absorption behavior of the nanofibers is directly identified in the cross-polarized images, which show band maxima at 45° azimuthal angle, in agreement with maximum in-plane p–s anisotropy for aligned nanofibers. The parallel-polarized Δ_{ss} phase image shows azimuthally rather homogeneous areas beside the vibrational band contributions. In such transparent regions, Δ_{ss} could potentially be used as a measure of optical thickness (the product of refractive index and thickness).⁴⁶

Figure 3b shows the azimuthal variation of the C–O–C band heights in the ss- and pp-polarized phase spectra as well as their difference. Classical FTIR polarimetry cannot measure absolute phases, but only relative ones. In contrast, IR-DCP can separate the information encoded in the polarization-dependent absolute phases.

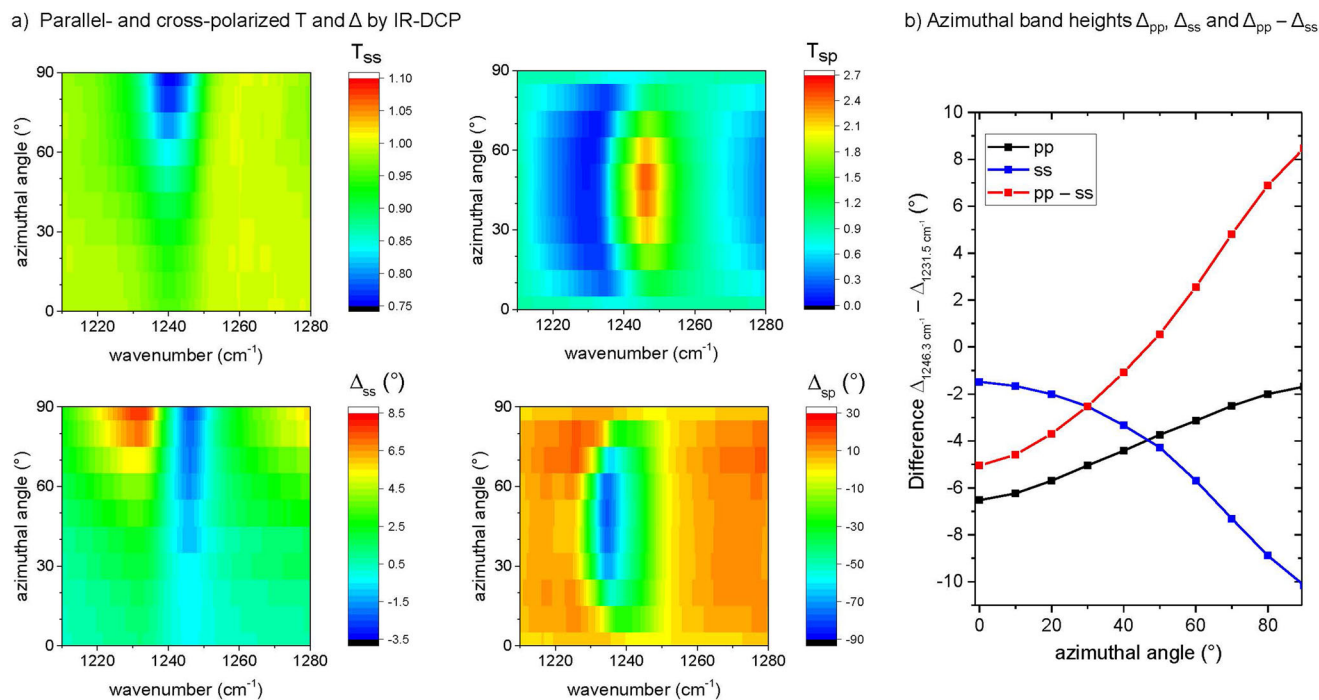


FIGURE 3 (a) Images of azimuthal ss- and sp-polarized infrared dual-comb polarimetry (IR-DCP) transmission and absolute phase spectra. T_{sp} exhibits a baseline value of 1 in the absence of anisotropy (e.g., for azimuthal sample rotations of 0° and 90°) due to the spectral normalization to a measurement without a sample. (b) Azimuthal variation of the C–O–C band height in the absolute ss- and pp-polarized phases as well as their difference

In summary, the spectral polarimetric amplitudes and phases simultaneously provide complementary information on sample structure and optical thickness. Moreover, IR-DCP acquires absolute phase data for arbitrary polarization configurations, allowing, for instance, the direct measurement of Δ_{sp} without the need for rotating optical elements such as polarizers. Fast sample imaging applications of parallel- and cross-polarized band amplitude and phase properties thus become available in the mid-IR spectral range.

Time characteristics

Figure 4a shows a time sequence of transmission and absolute phase spectra for the fiber scaffold obtained at a specific and constant polarimetric measurement setting (pp configuration at 45° sample azimuth).

These time-dependent images prove the high stability and robustness of the method in the shown time range for both transmission and absolute phase measurements. The integration time of a single spectrum (see Figure 4b) is 65 μs , plus a shot-to-shot delay of approximately 210 μs , giving a non-stroboscopic time resolution of approximately 275 μs . The time resolution can be pushed to as low as 1 μs with a zero shot-to-shot delay, with a trade-off of limiting the maximum measurement duration to 256 ms. The noise of the DC spectrometer in the second to sub-second time regime scales with the inverse of the square root of integration time⁴⁷; the signal-to-noise can therefore be improved by averaging multiple spectra. With its high time resolu-

tion for spectral monitoring in broad time windows from the min to μs range (with the potential of sub-microsecond time resolution⁴⁷), IR-DCP is currently a few orders of magnitude faster than reported for QCL-based IR laser polarimetry ($\approx 100 \text{ ms}/100 \text{ cm}^{-1}$).²⁹ The phase spectra show a weak overlaying interference. Its periodicity indicates a correlation with interferences of the 2 mm thick BaF_2 polarizers, possibly due to the slightly different optical paths in the sample and background measurement and small differences of the used polarizers and beamsplitters (e.g., weak heterogeneity or unevenness).

CONCLUSION AND OUTLOOK

IR-DCP was introduced as a new polarimetric technique for studies of anisotropic samples in the mid-IR spectral range. IR-DCP enables mid-IR polarimetric measurements of amplitudes and absolute phases at high spectral resolution (1.4 cm^{-1}). The method was applied to characterize a nanofiber scaffold with strong in-plane anisotropy. Azimuthal images of parallel- and cross-polarized dual-comb spectra were proven to be applicable for the direct inspection of anisotropic vibrational properties. Having with a single polarizer configuration access to both amplitudes and absolute phases offers new imaging prospects for cross-polarized sample properties.

Furthermore, IR-DCP provides sub-millisecond measurement times of 275 μs or less (potentially even sub-microsecond), limited by the repetition rate difference between FC1 and FC2.⁴⁷ The accessible integration times for noncyclic processes are far below those achievable

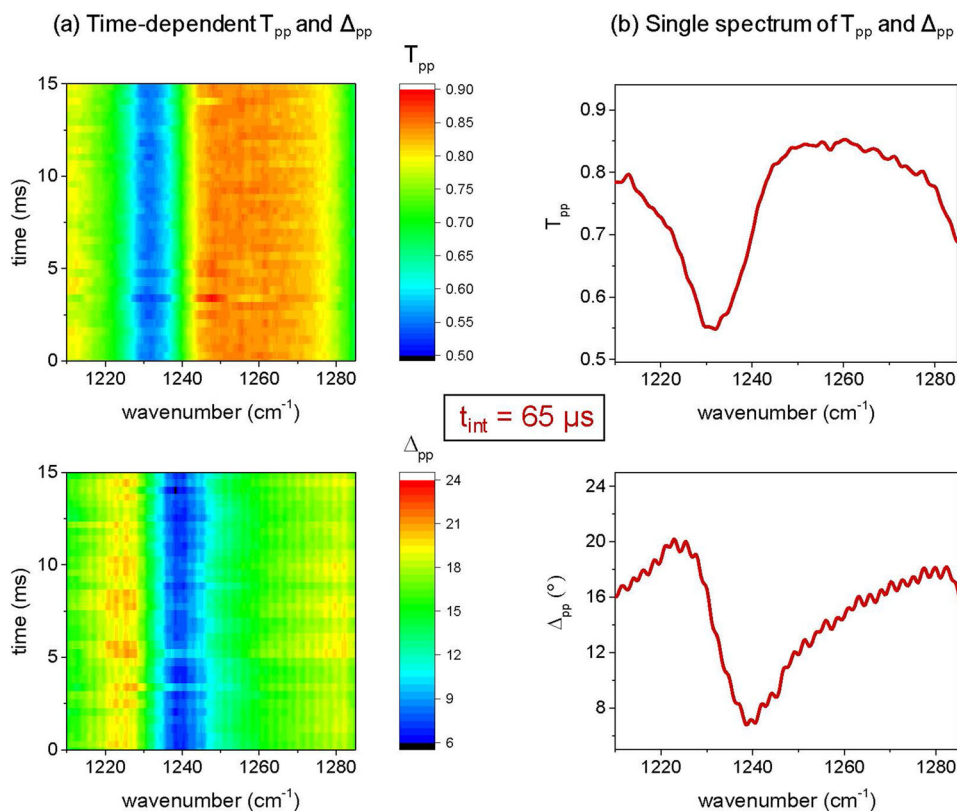


FIGURE 4 (a) Images of time-dependent T_{pp} and Δ_{pp} infrared dual-comb polarimetry (IR-DCP) spectra of the fiber scaffold at 45° azimuth. (b) The first single transmission and absolute phase spectrum with $65 \mu\text{s}$ integration time (t_{int}). The spectral resolution is 1.4 cm^{-1} .

with conventional FTIR techniques, thus enabling future applications regarding sub-millisecond resolved spectral investigations of irreversible or noncyclic variations of structural sample properties. The superior time resolution of IR-DCP compared with other IR approaches renders the method potentially interesting for many applications in photonics such as process control in the fabrication of waveguides and functional metasurfaces. In general, the novel time-resolved polarimetric possibilities could have a high potential scientific impact for previously unfeasible in situ and operando studies of irreversible or noncyclic processes or sample modifications. Further future applications of IR-DCP will also become available in other polarimetric measurement geometries.

In summary, the developed IR-DCP method has high potential for chemical and structural studies, for example, of anisotropic samples, growth processes, protein dynamics, phase transitions, chemical modifications, and reactions, which is relevant for material science, catalysis, biophysics, photonics, rheology, and metrology.

AUTHOR CONTRIBUTIONS

Conceptualization-lead; data curation-lead; investigation-equal; methodology-equal; resources-equal; validation-lead; visualization-lead; writing—original draft-lead; writing—review and editing-equal: Karsten Hinrichs. *Methodology-equal; resources-equal; writing—review and*

editing-supporting: Brianna Blevins. *Conceptualization-supporting; data curation-equal; investigation-supporting; methodology-equal; resources-supporting; validation-equal; visualization-equal; writing—original draft-supporting; writing—review and editing-equal:* Andreas Furchner. *Methodology-equal; resources-equal:* Nataraja Sekhar Yadavalli. *Methodology-equal; resources-equal; writing—review and editing-equal:* Sergiy Minko. *Conceptualization-supporting; data curation-equal; investigation-equal; methodology-equal; resources-equal; validation-equal; visualization-equal; writing—original draft-supporting; writing—review and editing-equal:* Raphael Horvath. *Conceptualization-supporting; data curation-supporting; investigation-equal; methodology-equal; resources-equal; validation-equal; visualization-equal; writing—original draft-supporting; writing—review and editing-equal:* Markus Mangold.

ACKNOWLEDGMENTS

The authors thank T. Shaykhtudinov for his scientific input and I. Engler and Ö. Savas for technical support. Financial funding is acknowledged: Bundesministerium für Bildung und Forschung; Die Regierende Bürgermeisterin von Berlin—Senatsverwaltung Wissenschaft, Gesundheit, Pflege und Gleichstellung; Ministerium für Innovation, Wissenschaft und Forschung des Landes Nordrhein-Westfalen; Federal Ministry of Education and Research (CatLab 03EW0015A/B); European Union (EFRE 1.8/13, Horizon 2020 grant 820419).

CONFLICTS OF INTEREST

The authors declare no conflicts of interest.

DATA AVAILABILITY STATEMENT

The data that support the findings of this study are available from the corresponding author upon reasonable request.

ETHICS STATEMENT

The authors confirm that they have followed the ethical policies of the journal.

ORCID

Karsten Hinrichs  <https://orcid.org/0000-0002-6580-7791>

PEER REVIEW

The peer review history for this article is available at <https://publons.com/publon/10.1002/ntls.20220056>.

REFERENCES

- He M, Folland TG, Duan J, et al. Anisotropy and modal hybridization in infrared nanophotonics using low-symmetry materials. *ACS Photonics*. 2022;9:1078-1095. doi:10.1021/acsp Photonics.1c01486
- Meng Y, Chen Y, Lu L, et al. Optical meta-waveguides for integrated photonics and beyond. *Light Sci Appl*. 2021;10:235. doi:10.1038/s41377-021-00655-x
- Yang H, Jussila H, Autere A, et al. Optical waveplates based on birefringence of anisotropic two-dimensional layered materials. *ACS Photonics*. 2017;4:3023-3030. doi:10.1021/acsp Photonics.7b00507
- Silva-Guillén JA, Canadell E, Guinea F, Roldán R. Strain tuning of the anisotropy in the optoelectronic properties of TiS_3 . *ACS Photonics*. 2018;5:3231-3237. doi:10.1021/acsp Photonics.8b00467
- Valderrabano M. Influence of anisotropic conduction properties in the propagation of the cardiac action potential. *Prog Biophys Mol Biol*. 2007;94:144-168. doi:10.1016/j.pbiomolbio.2007.03.014
- Street RA. The benefit of order. *Nat Mater*. 2006;5:171-172. doi:10.1038/nmat1601
- Lee S-J, Asheghali D, Blevins B, et al. Touch-spun nanofibers for nerve regeneration. *ACS Appl Mater Interfaces*. 2020;12:2067-2075. doi:10.1021/acsaami.9b18614
- Vitiello MS, Scali G, Williams B, De Natale P. Quantum cascade lasers: 20 years of challenges. *Opt Express*. 2015;23:5167-5182. doi:10.1364/OE.23.005167
- Hugi A, Horvath R, Jouy P. Advances of dual-comb spectroscopy based on QCL for environmental and water analysis. Proc. SPIE, Optical Fibers and Sensors for Medical Diagnostics, Treatment and Environmental Applications 2021, XXI, 1163511. 2021. doi:10.1117/12.2582911
- Hinrichs K, Shaykhtudinov T, Kratz C, Furchner A. Brilliant mid-infrared ellipsometry and polarimetry of thin films: toward laboratory applications with laser based techniques. *J Vac Sci Technol B*. 2019;37:060801. doi:10.1116/1.5122869
- Furchner A, Hinrichs K. Mid-infrared laser ellipsometry: a new era beyond FTIR. *Adv Opt Technol*. 2022;11:55-56. doi:10.1515/aot-2022-0013 Article ASAP
- Akhgar CK, Ramer G, Žbik M, et al. The next generation of IR spectroscopy: eC-QCL-based mid-IR transmission spectroscopy of proteins with balanced detection. *Anal Chem*. 2020;92:9901-9907. doi:10.1021/acs.analchem.0c01406
- Schwaighofer A, Brandstetter M, Lendl B. Quantum cascade lasers (QCLs) in biomedical spectroscopy. *Chem Soc Rev*. 2017;46:5903-5924. doi:10.1039/C7CS00403F
- Schönhals A, Kröger-Lui N, Pucci A, Petrich W. On the role of interference in laser-based mid-infrared widefield microspectroscopy. *J Biophotonics*. 2018;11:e201800015. doi:10.1002/jbio.201800015
- Consolino L, Cappelli F, de Cumis MS, De Natale P. QCL-based frequency metrology from the mid-infrared to the THz range: a review. *Nanophotonics*. 2019;8:181-204. doi:10.1515/nanoph-2018-0076
- Galán-Freyte NJ, Pacheco-Londoño LC, Román-Ospino AD, Hernandez-Rivera SP. Applications of quantum cascade laser spectroscopy in the analysis of pharmaceutical formulations. *Appl Spectrosc*. 2016;70:1511-1519. doi:10.1177/0003702816662609
- Wei S, Kulkarni P, Ashley K, Zheng L. Measurement of crystalline silica aerosol using quantum cascade laser-based infrared spectroscopy. *Sci Rep*. 2017;7:13860. doi:10.1038/s41598-017-14363-3
- Hinrichs K, Shaykhtudinov T. Polarization-dependent atomic force microscopy-infrared spectroscopy (AFM-IR): infrared nanopolarimetric analysis of structure and anisotropy of thin films and surfaces. *Appl Spectrosc*. 2018;72:817-832. doi:10.1177/0003702818763604
- Dazzi A, Prater CB. AFM-IR: technology and applications in nanoscale infrared spectroscopy and chemical imaging. *Chem Rev*. 2017;117:5146-5173. doi:10.1021/acs.chemrev.6b00448
- Wehmeier L, Lang D, Liu Y, et al. Polarization-dependent near-field phonon nanoscopy of oxides: SrTiO_3 , LiNbO_3 , and $\text{PbZr}_{0.2}\text{Ti}_{0.8}\text{O}_3$. *Phys Rev B*. 2019;100:035444. doi:10.1103/PhysRevB.100.035444
- Yao Z, Chen X, Wehmeier L, et al. Probing subwavelength in-plane anisotropy with antenna-assisted infrared nano-spectroscopy. *Nat Commun*. 2021;12:2649. doi:10.1038/s41467-021-22844-3
- Tong L, Huang X, Wang P, et al. Stable mid-infrared polarization imaging based on quasi-2D tellurium at room temperature. *Nat Commun*. 2020;11:2308. doi:10.1038/s41467-020-16125-8
- Xu S, Rowlette J, Lee YJ. Imaging 3D molecular orientation by orthogonal-pair polarization IR microscopy. *Opt Express*. 2022;30:8436-8447. doi:10.1364/OE.449667
- Freitag S, Baer M, Buntzoll L, et al. Polarimetric balanced detection: background-free mid-IR evanescent field laser spectroscopy for low-noise, long-term stable chemical sensing. *ACS Sensors*. 2021;6:35-42. doi:10.1021/acssensors.0c01342
- Lüdeke S, Pfeifer M, Fischer P. Quantum-cascade laser based vibrational circular dichroism. *J Am Chem Soc*. 2011;133:5704-5707. doi:10.1021/ja200539d
- Bakir G, Girouard BE, Wiens R, et al. Orientation matters: polarization dependent IR spectroscopy of collagen from intact tendon down to the single fibril level. *Molecules*. 2020;25:4295. doi:10.3390/molecules25184295
- Furchner A, Kratz C, Rappich J, Hinrichs K. Multi-timescale infrared quantum cascade laser ellipsometry. *Opt Lett*. 2022;47:2834-2837. doi:10.1364/OL.457688
- Ebner A, Zimmerleiter R, Hingerl K, Brandstetter M. Towards real-time in-situ mid-infrared spectroscopic ellipsometry in polymer processing. *Polymers*. 2022;14:7. doi:10.3390/polym14010007
- Furchner A, Kratz C, Hinrichs K. Sub-second infrared broadband-laser single-shot phase-amplitude polarimetry of thin films. *Opt Lett*. 2019;44:4387-4390. doi:10.1364/OL.44.004387
- Picqué N, Hänsch TW. Frequency comb spectroscopy. *Nat Photonics*. 2019;13:146-157. doi:10.1038/s41566-018-0347-5
- Sumihara KA, Okubo S, Okano M, Inaba H, Watanabe S. Polarization-sensitive dual-comb spectroscopy. *J Opt Soc Am B*. 2017;34:154-159. doi:10.1364/JOSAB.34.000154
- Minamikawa T, Hsieh YD, Shibuya K, et al. Dual-comb spectroscopic ellipsometry. *Nat Commun*. 2017;8:610. doi:10.1038/s41467-017-00709-y

33. Röseler A, Korte EH. In: Chalmers JM, Griffiths PR, eds. Chap. 2.8 in *Handbook of Vibrational Spectroscopy*. John Wiley & Sons; 2001.
34. Menzel C, Rockstuhl C, Lederer F. Advanced Jones calculus for the classification of periodic metamaterials. *Phys Rev A*. 2010;82:053811. doi:[10.1103/PhysRevA.82.053811](https://doi.org/10.1103/PhysRevA.82.053811)
35. Villares G, Hugi A, Blaser S, Faist J. Dual-comb spectroscopy based on quantum-cascade-laser frequency combs. *Nat Commun*. 2014;5:5192. doi:[10.1038/ncomms6192](https://doi.org/10.1038/ncomms6192)
36. Coddington I, Newbury N, Swann W. Dual-comb spectroscopy. *Optica*. 2016;3:414-426. doi:[10.1364/OPTICA.3.000414](https://doi.org/10.1364/OPTICA.3.000414)
37. Norahan MJ, Horvath R, Woitzik N, et al. Microsecond-resolved infrared spectroscopy on nonrepetitive protein reactions by applying caged compounds and quantum cascade laser frequency combs. *Anal Chem*. 2021;93:6779-6783. doi:[10.1021/acs.analchem.1c00666](https://doi.org/10.1021/acs.analchem.1c00666)
38. Jouy P, Wolf JM, Bidaux Y, et al. Dual comb operation of $\lambda \sim 8.2 \mu\text{m}$ quantum cascade laser frequency comb with 1 W optical power. *Appl Phys Lett*. 2017;111:141102. doi:[10.1063/1.4985102](https://doi.org/10.1063/1.4985102)
39. Pinkowski NH, Biswas P, Shao J, Strand CL, Hanson RK. Thermometry and speciation for high-temperature and -pressure methane pyrolysis using shock tubes and dual-comb spectroscopy. *Meas Sci Technol*. 2021;32:125502. doi:[10.1088/1361-6501/ac22ef](https://doi.org/10.1088/1361-6501/ac22ef)
40. Muñoz-Pineda E, Järrendahl K, Arwin H, Mendoza-Galván A. Symmetries and relationships between elements of the Mueller matrix spectra of the cuticle of the beetle *Cotinis mutabilis*. *Thin Sol Films*. 2014;571:660-665. doi:[10.1016/j.tsf.2013.11.144](https://doi.org/10.1016/j.tsf.2013.11.144)
41. Hinrichs K, Eichhorn K-J, eds. Chap. 1, 2, 3, 6, 7, 9, 12, 13, 19, 20, 21, 22 in *Ellipsometry of Functional Organic Surfaces and Films*. 2nd ed. Springer Ser. Surf. Sci. 52, Springer International Publishing AG; 2018.
42. Gorodzha SN, Surmeneva MA, Surmenev RA. Fabrication and characterization of polycaprolactone cross-linked and highly-aligned 3-D artificial scaffolds for bone tissue regeneration via electrospinning technology. *Mater Sci Eng*. 2015;98:012024. doi:[10.1088/1757-899X/98/1/012024](https://doi.org/10.1088/1757-899X/98/1/012024)
43. Hinrichs K, Blevins B, Furchner A, Yadavalli NS, Minko S. Infrared polarimetry: anisotropy of polymer nanofibers. *Micro Nano Eng*. 2022;14:100116. doi:[10.1016/j.mne.2022.100116](https://doi.org/10.1016/j.mne.2022.100116)
44. Wang Z, Sun B, Lu X, Wang C, Su Z. Molecular orientation in individual electrospun nanofibers studied by polarized AFM-IR. *Macromolecules*. 2019;52:9639-9645. doi:[10.1021/acs.macromol.9b01778](https://doi.org/10.1021/acs.macromol.9b01778)
45. Furchner A, Hinrichs K. Crosspolarization with imperfect infrared polarizers. *Thin Solid Films*. 2022;763:139560. doi:[10.1016/j.tsf.2022.139560](https://doi.org/10.1016/j.tsf.2022.139560)
46. Arwin H. In: Tompkins HG, Irene EA, eds. *Handbook of ellipsometry*. William Andrews; 2005:808.
47. Klocke JL, Mangold M, Allmendinger P, et al. Single-shot sub-microsecond mid-infrared spectroscopy on protein reactions with quantum cascade laser frequency combs. *Anal Chem*. 2018;90:10494-10500. doi:[10.1021/acs.analchem.8b02531](https://doi.org/10.1021/acs.analchem.8b02531)

How to cite this article: Hinrichs K, Blevins B, Furchner A, et al. Mid-infrared dual-comb polarimetry of anisotropic samples. *Nat Sci*. 2023;3:e20220056.
<https://doi.org/10.1002/ntls.20220056>